Cell-to-module losses in standard crystalline PV modules – An industrial approach

Eduardo Forniés, Aurinka PV Group SL, Madrid, & **José Pedro Silva**, CIEMAT – División de Energías Renovables, Madrid, Spain

ABSTRACT

One of the main concerns of module manufacturers is the power loss that takes place when the solar cells are incorporated in PV modules. This power loss, known as *cell-to-module (CTM) loss*, results from the influence of many factors which occur during module production. Some of these factors lead to a gain in power at the end of the process; on the other hand, some are responsible for a loss of power and offset the positive effects of other ones, resulting in a net power loss. In this paper the CTM losses will be addressed from an industrial point of view and for standard crystalline PV modules. The focus will first be on some of the most frequent issues detected in production lines and their influence on module power loss. More extensive research is then carried out to arrive at an explanation of their origin. This paper describes some of the mentioned factors along with the different ways of detecting them.

Introduction

During the last few decades the producers of PV modules have reduced their costs, thus contributing to making PV energy a realistic option for obtaining not only clean but also profitable energy. This cost reduction has been addressed using different approaches: improving solar cell efficiencies, reducing material costs, optimizing production processes, etc. Among these, the reduction of the gap that exists between cell power and module power is being studied by many researchers; Haedrich et al. [1], in particular, have done an interesting overview of all of these investigations. The power gains and losses occurring in the module are classified as follows:

- **Optical losses:** due to glass reflection and absorption, encapsulant reflection and absorption [2], and shading of tabbing ribbon.
- **Optical gains:** due to refractive index matching between encapsulant and anti-reflection coating (ARC), and the back reflection of light rays from the fingers, tabbing ribbon, cell area and cell spacing area (backsheet reflection) [3,4].
- **Electrical losses:** due to an increase in series resistance (R_s) and contact resistance [5] generated from string formation and cable assembly.
- **Mismatch losses:** due to a scattering of the electrical parameters of solar cells [6,7].

This paper will focus on the causes of different events along the PV module

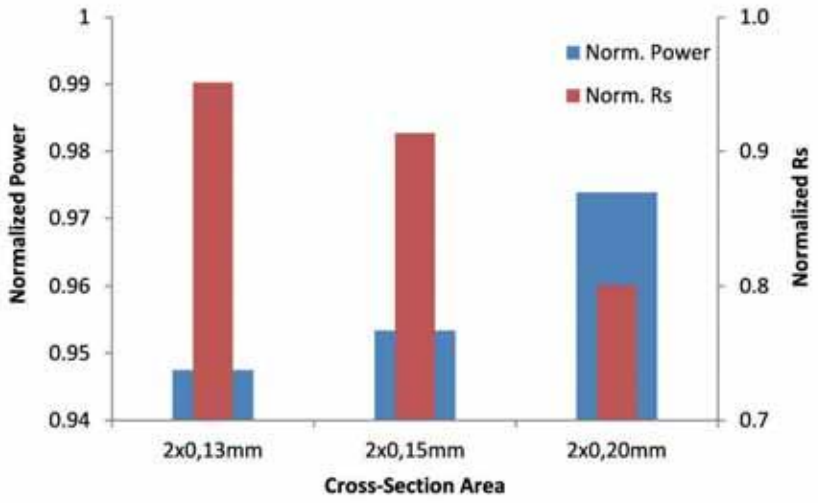

Figure 1. Module power and series resistance vs. tabbing ribbon thickness.

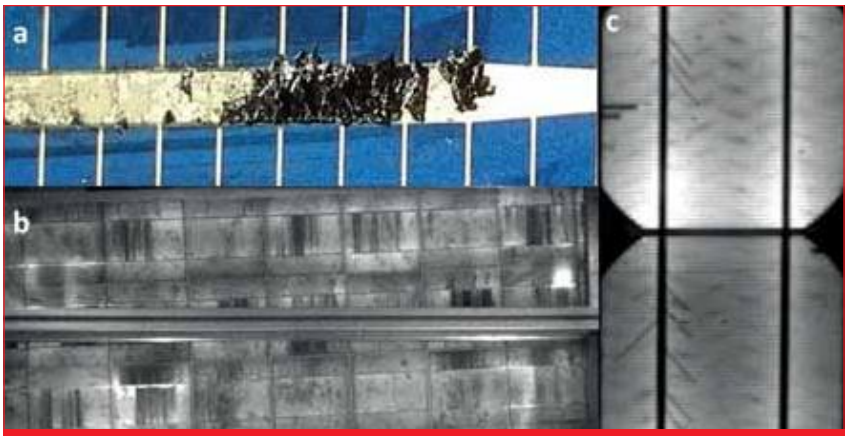

Figure 2. Effects of crystal damage: (a) view of the solar cells affected by crystal damage after the peeling test; b) EL image of a module with several cells affected by crystal damage; (c) V-shape breakage patterns of single-crystal solar cells, caused by shear stress after the soldering process.

production chain that give rise to CTM losses/gains and how they can be addressed.

"The reduction of the gap that exists between cell power and module power is being studied by many researchers."

CTM losses due to cell interconnection

Ribbon and cell design

In standard module manufacturing, once the solar cells have been classified they are soldered to make a series connection between them. This is performed by connecting the negative side of one cell with the positive side of the adjacent cell. For making that contact, a copper tabbing ribbon, coated with an alloy of Sn/Pb (or Ag/Sn/Pb), is used. There is a distinct increase in R_s because of the tabbing ribbon to cell interconnection process, but this resistance can be reduced by increasing either the number of busbars or the cross section of the tabbing ribbon.

Adding busbars

The addition of more busbars to the cells increases the number of collectors for current transport through the module, thus reducing the current density per busbar. Nowadays, for a 156mm × 156mm cell, the standard number of buses is three; however, some new technologies, which can achieve efficiencies of up to 19–22%, use a higher number of buses – in some cases up to five. New interconnection concepts, such as smart wiring, are being developed, but are not yet fully integrated in the industry.

Increasing the number of busbars introduces additional shadowing of the cell, consequently reducing the photogenerated current. This effect is minimized by a higher charge-carrier transport efficiency, as the charge carriers have to travel less distance through the cell to reach a collector, thus leading to a net increase in efficiency up to a point where the busbar shadowing predominates over the influence of current transport [8].

Increasing tab–ribbon cross section

Increasing the width of the tabbing ribbon [5] reduces the R_s of the module, but extends the shadow projected on the cell surface; the width can therefore be increased up to a certain point, always taking into consideration the width of the cell buses. The next option is to increase the thickness of the tabbing ribbon. In the last ten years the thickness has been increased from 0.12mm to 0.23mm (or higher), as the efficiency and size of the cells demanded a greater tabbing ribbon cross section to extract the maximum power available in the cells. Consequently, the power output of modules increased as a direct result of the reduction in R_s.

To clarify the influence of tabbing ribbon thickness on power output, 82 modules were manufactured with the

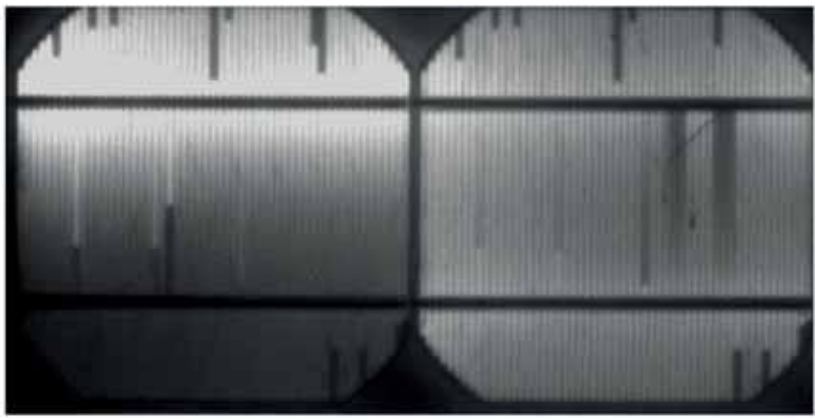

Figure 3. EL image of a module affected by an unsoldered tabbing ribbon – the cell affected is on the left side. The lower busbar is unsoldered and shows up as a dark busbar, whereas the upper busbar, which is forced to transport all the module current, appears brighter.

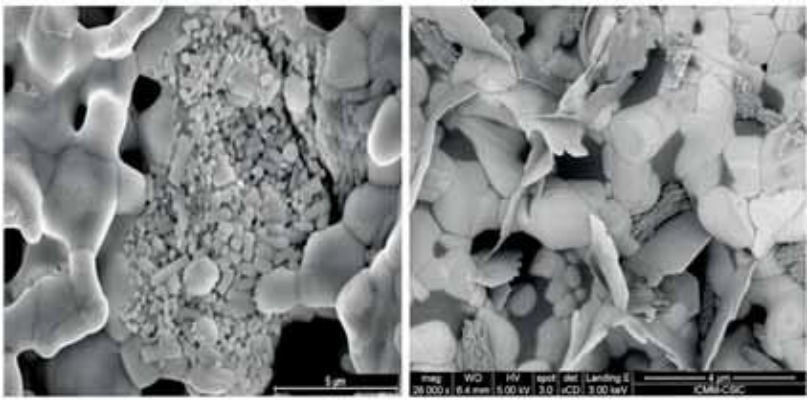

Figure 4. Scanning electron microscope (SEM) images of front busbars that presented adherence failure in the peel test. Formations different from those of a silver microstructure can be observed.

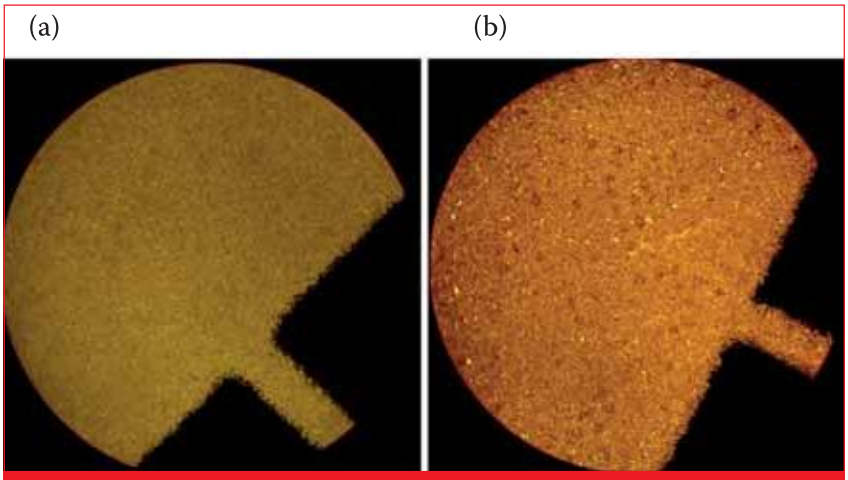

Figure 5. (a) Optical microscope image of a normal front busbar. (b) A front busbar affected by bright spots.

same materials and solar cells. Multicrystalline solar cells of dimension 156mm × 156mm and two busbars were assembled in a 10 × 6 configuration; the solar cell efficiency was the same for all the modules. Three different tabbing ribbon thicknesses were used in the experiment. Fig. 1 shows the average power and R_s of the modules: the average power has been normalized to the sum of the nominal power of 60 cells, and R_s has been normalized to the maximum R_s. An increase in module power inversely proportional to the series resistance was obtained experimentally.

The thickness of tabbing ribbon nevertheless has a direct influence on the silicon just below the bus: because of the different thermal expansion coefficients (TECs) of copper and silicon, breakages occur during the soldering process, leading to what is called *crystal damage*, as shown in Fig. 2(a). This defect can result in a serious lack of contact, which is exacerbated during thermal cycling once the module has been installed. If the crystal damage is extensive, it can easily be detected by electroluminescence (EL) imaging (Fig. 2(b)), and the module rejected; however, if the defect does not extend very far, the module may pass the quality controls and then be installed. In this situation, under outdoor thermal cycling, the module may be subjected to a high power loss due to the propagation of the defect. To counteract this effect the yield strength of the tabbing ribbon has been reduced from 90N/m to 30N/m, reducing the crystal damage, also known as *rip-out*.

It has been observed that multicrystalline silicon solar cells are more susceptible to this defect, while single-crystal solar cells, under high shear stress, tend to break in a V-shape fracture, as seen in Fig. 2(c).

Mismatch

The dispersion in the electrical parameters of solar cells (also known as *mismatch)*, and its relation to relative power loss (RPL) when the cells are associated in series to form a module, have also been widely studied [9–14]. Recent work [6,7] has shown that under standard cell classifications, the RPL, although it exists, is below the detection limits of solar simulators. This could lead to a re-evaluation of cell sorting: for example, cell classification may be carried out using wider ranges of electrical parameters to improve production yields. In module production environments it would no longer be recommended to sort 100% of the cells, resulting in savings in the capex and the breakages associated with this practice. However, it is advisable to perform at least the measurement of a certain population of cells as a quality control. Nevertheless, during module production, the manufacturer may follow certain practices that deviate from the standard production process, leading to an increase in RPL due to mismatch.

> "The tabbing–stringing process is the most critical process of module production in terms of failures."

Soldering

The tabbing–stringing process (soldering the solar cells to each other) is the most critical process of module production in terms of failures. During soldering, the solar cells are subjected to high thermal shear stress [5,15,16]; as a result, most manufacturing failures occur during this process. The following sections discuss

different failure modes and explanations of why these occur, derived from direct experience and research in industrial environments.

Adhesive failure between tabbing ribbon and busbar

The contact resistance also affects the overall module series resistance. Problems related to contact resistance mainly take place at the silicon–busbar interface and at the busbar–tabbing ribbon interface. As regards the busbar–tabbing ribbon interface, the contact failures occur during the soldering process. For example, bad storage conditions of solar cells or a prolonged period of time that the cells are on the production line without encapsulation can lead to the creation of an oxide film on top of the busbar; this reduces the soldering effectiveness and consequently leads to a lack of contact or even a complete peeling of the ribbon.

The flux is also a direct agent, which plays an important role during soldering. An eventual clogging of the flux dispensers leaves the cell buses without flux just before soldering. This gives rise to unsoldered cells in the module, which translates to a loss of power (Fig. 3). In this case, the current generated by the module is forced to pass through the soldered buses, which leads to a brighter appearance under EL testing (upper busbar in Fig. 3).

In the case of problems arising from solar cell manufacturing, contaminants in silver paste have a strong influence. A poor-quality silver paste, in which elements different from those related to glass frit formation or conductivity purposes are present, may have a negative effect upon the adherence strength of both cell and tabbing ribbon. In Fig. 4, different solar cells originating from failing lots in the soldering process were analysed. Several microstructures were detected, of which the main components were metal oxides. The soldering failures derived from those structures were not only adhesive but also cohesive.

The most common way of carrying out contact deposition is the screen-printing process, in which the silver paste of the front and back contacts is printed onto the silicon. After the printing, the solar cells are subjected to a thermal process that is responsible for triggering the drive-through of the silver through the ARC. If the thermal process is not done correctly, the coalescence of silver grains may occur and pure silver flakes are formed on the busbar surface; these flakes are called *bright spots* because of their brightness when exposed to light. Aurinka PV Group inspected a batch of solar cells from the same manufacturer and the same lot; some of these were found to have the bright spots (Fig. 5(b)). During solar simulator testing, modules with affected cells demonstrated 3% less power than those made from 'normal' cells.

After automatic soldering, an adherence test was carried out. The

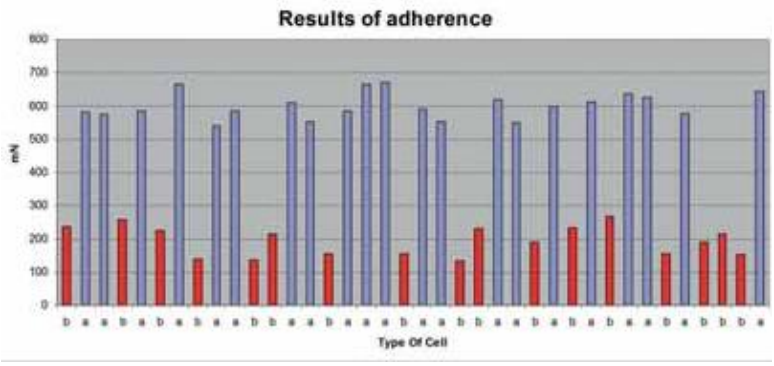

Figure 6. Red columns: adherence test carried out on cells affected by bright spots (see Fig. 5(b)). Blue columns: adherence test results for cells without bright spots (see Fig. 5(a)) from the same lot.

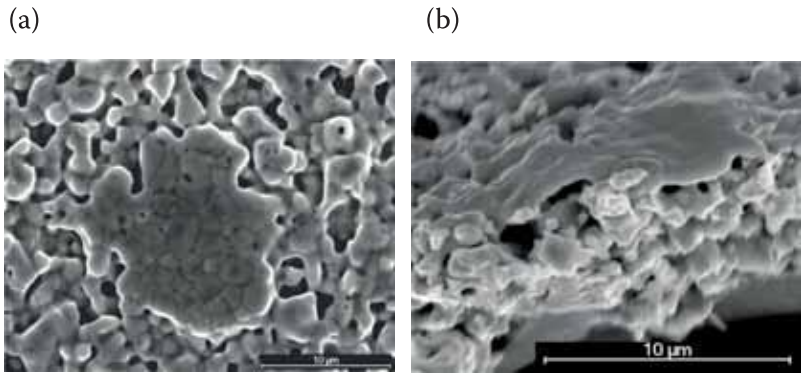

Figure 7. (a) Surface SEM picture of the microstructure of one 'bright spot.' (b) Tilted SEM picture of a busbar cut through a bright spot.

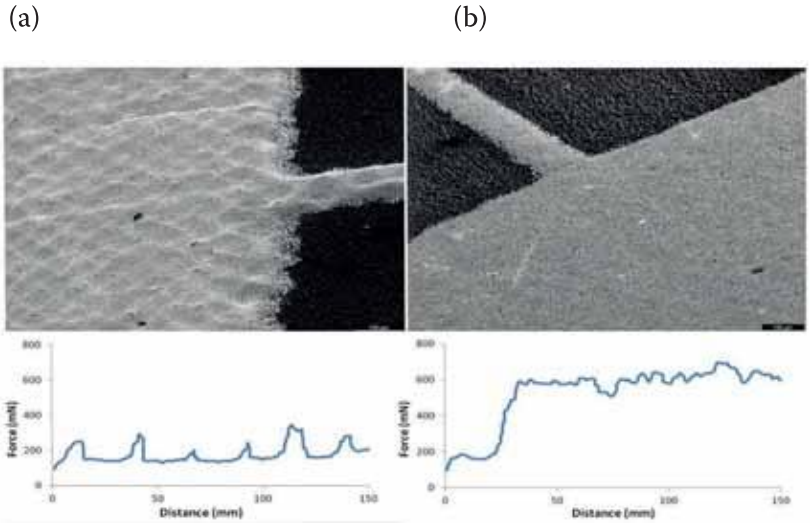

Figure 8. (a) SEM image of a front busbar with the topography derived from the mesh of the screen-printing process (top), and the corresponding adherence test result for one of the soldered buses (bottom). (b) SEM image where the mesh topography is absent (top), and the corresponding adherence test result for one of the soldered buses (bottom).

results, presented in Fig. 6, reveal the poor adhesion of cells with bright spots in comparison with those not affected by this issue.

For a more detailed explanation of the problem, the cells were inspected using a scanning electron microscope (SEM). The flake-shaped grains that have formed on top of the busbar have a softer surface than the silver paste surrounding them (Fig. 7); this makes the reflection of light more intense, resulting in the appearance of bright spots. An energy dispersive X-ray (EDX) analysis revealed that those grains are surface structures formed by pure silver (Ag), whereas the area surrounding them is mainly formed by silver as well as other metals and oxygen. The adherence of the tabbing ribbon onto the silver busbars depends on the number of flakes per mm^2. Because of the flat area of the flakes, there is a detrimental effect on adherence.

Changes in silver paste composition, busbar design or the mechanical parameters of the tabbing ribbon have a strong influence on the soldering process. The composition of silver pastes as well as the busbar geometry and distribution is under ongoing development in order to improve solar cell efficiencies and to reduce production costs. Nevertheless, any modifications to solar cell elements, although necessary, need to be realized in full collaboration with module producers, as the changes may have a direct effect on module performance and manufacturing processes.

Concerning busbar geometry, because of the soaring price of silver, solar cells producers have found different ways of saving silver by making discontinuous busbars, which also affect the soldering process. On the one hand, the solderability of silver pads is affected for many reasons: different contact pressures for silver pads than for aluminium (in rear buses) or for silicon (in front buses); inhomogeneous distribution of heat along the busbars; inhomogeneous distribution of shear stress; and so on. On the other hand, because of discontinuities the contact area is reduced. Although it has been reported that the contact resistance between the tabbing ribbon and the cell is constant and negligible in the case of sufficient solder spots having been achieved [17], the fact that the soldering process window narrows must be taken into account.

The composition or viscosity of the silver paste also affects the soldering. Around six years ago, there used to be Al in the silver paste composition for the back buses, which enhanced the solderability of the tabbing ribbon onto the back busbar; however, Al is no longer present in the back buses, causing a reduction in solderability as well as in the soldering process window. Some manufacturers are trying to reduce, or even eliminate, the Pb content in silver pastes in order to meet future environmentally friendly requirements. Normally those new silver pastes use Bi as an alternative to Pb, but this replacement of Pb by Bi also has an influence on the soldering process, leading to a decrease in adhesion force.

Regarding silver paste viscosity, a correlation between the macroscopic topography of the busbar and the adhesion has also been detected. The topography of fired silver paste is determined by paste properties (viscosity, emulsion thickness, etc.) and screen dimensions (i.e. wire diameter of the mess). During in-line quality control of the soldering process (peel test), an adhesion failure was detected in a certain lot of cells from the same supplier (Fig. 8, bottom left). The topography of a group of cells, with good and bad results during the peel test, was analysed by SEM: the difference between them shows up very clearly (Fig. 8, top). A distinct topography with a mesh-shaped pattern (arising from the mesh of the screen-printing process) is present in those cells that suffered adhesion failure, while the busbar surface of 'good' cells appears to be flat and soft. Several modules were manufactured using solar cells that demonstrated the above-mentioned busbar patterned topography and using solar cells with a soft busbar surface. The materials used and the soldering conditions were the same. The modules affected by the pattern issue produced 2% less power than those made using 'normal' cells.

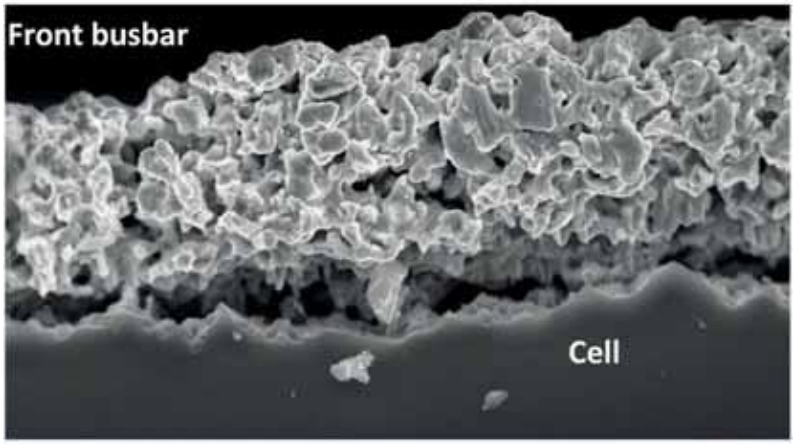

Figure 9. Front busbar of a cell affected by a bad contact: total delamination is observed.

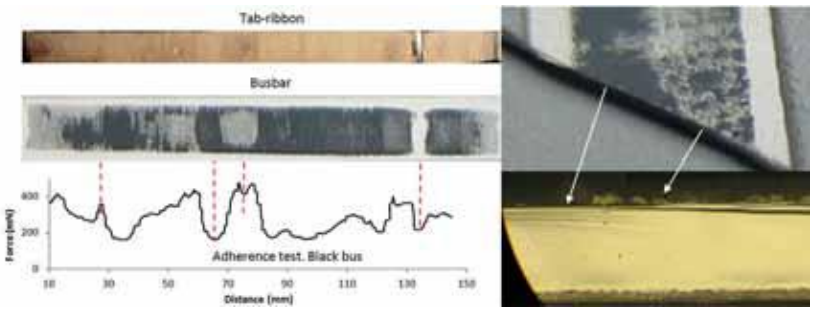

Figure 10. Top left: inner part of the tabbing ribbon after the peel test. Middle left: busbar of a cell exhibiting the 'black bus' effect after the peel test. Bottom left: peel force vs. busbar length. Top right: section view of the busbar after the peel test. Bottom right: optical microscope section view of the same busbar – the absence of silver in the black area is evident.

Busbar-to-cell adhesive failure

The adhesion force between the silver paste and the cell is also an important factor that influences the final CTM losses. The origins of this kind of failure are diverse: poor-quality silver paste, inefficient drying or co-firing processes in solar cell production, storage of wafers in bad conditions, inappropriate handling of silicon wafers, etc. All of

these result in deficient contact between cell and silver paste, and can even lead to busbar flaking, as shown in Fig. 9.

Eventually, in some of the steps of solar cell production prior to screen printing, the wafer surface may sustain some kind of contamination (oxide, fingerprints, etc.). Subsequently, at the end of the manufacturing process, the solar cells are produced with an undesirable interlayer between the busbar and the cell, which creates a higher contact resistance. The performance of a cell, however, may be good enough for it to be commercialized, and it therefore proceeds to module manufacturing. In this case, the adhesive failure occurs during the soldering process, where, although the adherence between the busbar and the tabbing ribbon is high, the peel test fails as a result of the complete detachment of the silver busbar from the cell. Thus, the area of the busbar turns dark in colour; this effect is commonly known as *black bus* or *dark bus*.

This problem has been detected by Aurinka in the solar cells of many suppliers. During module production, the 'black bus' effect appears as a failure in the peel test, where the adherence (peel force) exhibits very low values. Additionally, all the busbar's silver paste is removed, in a clear adhesive failure, in those areas where the dark colour appears. In the case of acceptable peel-test results, the peeled tabbing ribbon removes part of the busbar as a result of a cohesive 'failure' deliberately provoked by the peel force. Nevertheless, the cohesive 'failure' leaves a grey colour, and high adhesive values. A white colour appearance on the busbar surface means that no soldering has been performed and consequently the adhesion is also very low. Fig. 10 shows all the failure types described above, simultaneously in the same busbar, along with the adherence test results. The tabbing ribbon after the peel test is also presented. It is clearly shown that where a dark area appears, the peel force is very low, confirming the existence of an adhesive failure. One of the cells was inspected by optical microscope after the peel test. In the section view (Fig. 10, bottom right), it can be observed that no silver paste remains in the silicon where the black area appears (left arrow), whereas in the grey areas (where a cohesive 'failure' occurred), some silver remains (right arrow) and the peel force is much higher.

The lot of cells that exhibited this problem was electrically measured and compared with another lot from the same supplier having the same efficiency (Fig. 11). As can be deduced from the graph, the lot afflicted by the 'black bus' effect presents a very high scattering of R_s in its cells, with R_s values of up to 20mΩ, well above the standard 4–8mΩ. The inset in Fig. 11 shows, as final evidence of the existence of a contamination interlayer, a fingerprint on one of the affected cells after the peel test.

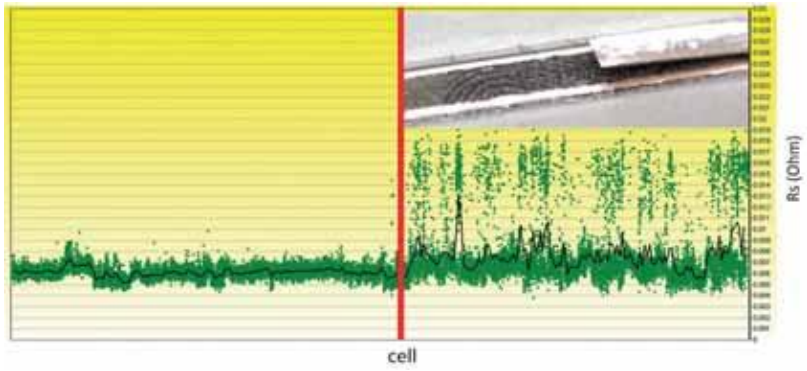

Figure 11. Series resistances of the cells suffering from the black bus effect (right) compared with cells without this failure from the same supplier and with the same efficiency (left).

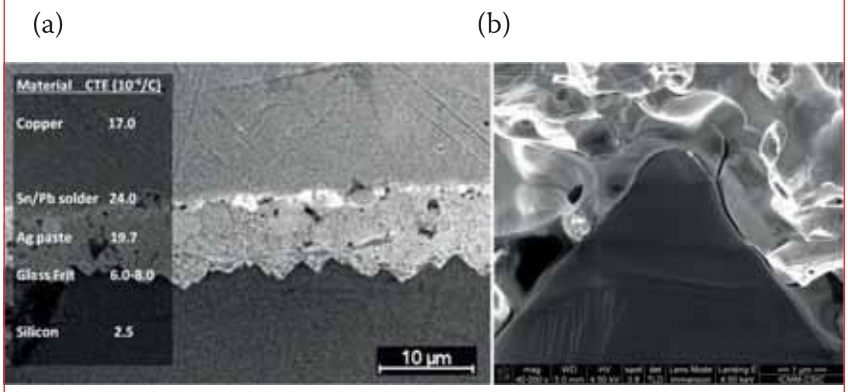

Figure 12. (a) SEM section view of one soldered solar cell: tabbing ribbon, front busbar and silicon are shown, and the CTEs are specified in the inset. (b) SEM section view of a fracture in the glass of a solar cell.

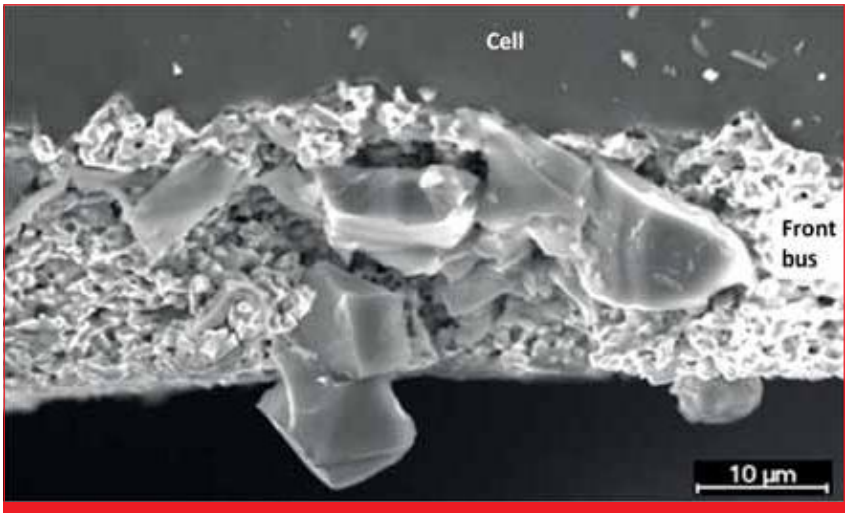

Figure 13. Example of bulk contamination of a front busbar.

"The average power of modules affected by the black bus effect was 3.8% lower than that of modules not exhibiting the failure."

4th International Off-Grid Lighting Conference and Exhibition

October 26-29, 2015
Dubai, United Arab Emirates

The premier global event for the **off-grid solar energy and lighting industry**

October 26-29, 2015, Dubai, United Arab Emirates

- **600+ conference participants and 80+ exhibitors**
- **A dedicated day for topical side events organised by participants**
- **With keynote speech from Professor Muhammad Yunus, Nobel Laureate**

Among others, high level speakers include:

- The Rt Hon Grant Shapps, UK Minister of State for International Development
- Dr. Kandeh Yumkella, Special Representative of the UN Secretary General and CEO of Sustainable Energy for All
- Anita George, Senior Director, Energy and Extractive Industries Global Practice, World Bank Group

The conference focuses on:

- Business Services
- The role of governments and policy in facilitating market growth
- Technical and quality assurance
- Social and environmental impacts

An exhibition and trade fair running in tandem with the conference will enable:

- An exchange between 80+ exhibitors
- Business-to-business networking opportunities

Book your tickets and exhibition space for THE premier global event for the off-grid solar energy and lighting industry at www.conference2015.gogla.org

Presented by

Sponsored by

Platinum sponsor

Sliver sponsor

Bronze sponsor

Supported by

All the modules produced with both lots of cells were measured under standard test conditions (STC). The results show that the average power of modules affected by the black bus effect was 3.8% lower than that of modules not exhibiting the failure.

With regard to the nature of all the interfaces involved in solar cell interconnection, it is important to take into account the difference between the coefficients of thermal expansion (CTEs) of the different interfaces that participate in the soldering. Fig. 12(a) is an SEM photograph of a section view of a soldered solar cell. In this image all the interfaces are displayed and the CTE of each material is also indicated (CTEs were extracted from Moyer et al. [18]). From Fig. 12 it can be inferred that the solder strongly smears throughout the interface area because the thickness of the solder decreases from 15–20 microns down to a few microns. It is likely that a combination of temperature and the pressure of the tabber–stringer pins on the tabbing ribbon cause the thinning of the solder. An EDX analysis of the interface compositions confirms the composition shown in the inset of Fig. 12(a).

As reported by Moyer et al. [18], the largest change in CTEs takes place at the silicon–glass and glass–Ag interfaces, which means that, during thermal processes, the residual stress is concentrated mainly at those interfaces. As a consequence of silver paste components and the parameters of the firing process, a thick glass interface may be formed. When the solar cell is subjected to the thermal stress of the soldering process, the resulting shear stress can cause the glass to fracture. As a result, an adhesive failure of the silver busbar and the solar cell occurs and the known black bus effect may appear. Fig. 12(b) shows a fracture in the glass of a single-crystal solar cell after soldering.

Cohesive failure of the busbar due to silver paste

Leach resistance is strongly related to the cohesive properties of the busbar. The silver paste components can be separated into 1) inorganic – glass frit, Ag powder and oxides, and 2) organic – solvent, resin and organic additives. The inorganic components are responsible for adhesion and leach resistance [18], whereas unusual proportions of organic additives may be detrimental to these properties. Nevertheless, the organic components are responsible for the green strength of the silver paste, which, combined with the parameters of the drying and firing processes, may cause a loss of integrity of the busbar, translating into a lack of cohesion. On the other side, foreign microstructures formed by contaminants are also responsible for cohesive failure, as they replace the glass matrix and Ag particles that primarily constitute the busbars. Fig. 13 shows a readily apparent bulk contamination of the silver paste once it has been printed onto the solar cell.

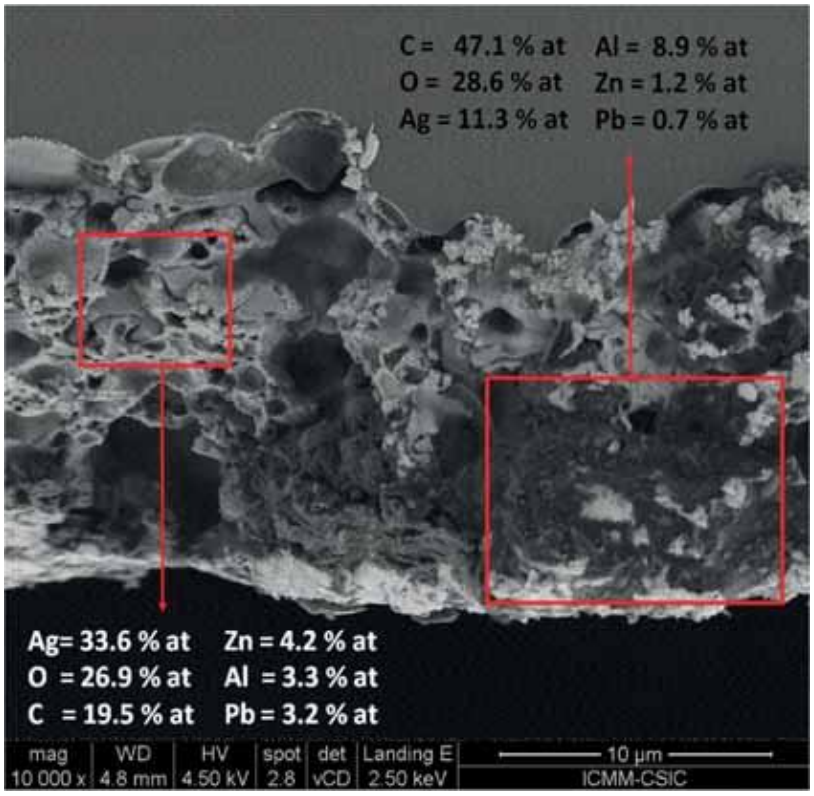

Figure 14. EDX analysis of two different areas of a front silver paste. In the dark areas, a prominent peak of Al is detected, while the bright areas correspond mainly to Ag.

In another sample investigation that took place in an industrial environment, a massive cohesive failure was observed in solar cells where the front busbars presented high concentrations of C and O, as well as Al as a contaminant; the latter is extremely rare and potentially harmful as a possible origin of shunt formations due to Al spiking. As usual, after the peel-test failure the cells were inspected in the laboratory. An SEM and EDX analysis was carried out on the solar cells, and Al was found in the bulk of the silver paste (Fig. 14).

Optical gains/losses

Once solar cells have been encapsulated, there are losses related to optical principles. Before the radiation reaches the cell, reflections at the air–glass and glass–encapsulant interfaces occur as well as absorption by the glass and encapsulant [2]. As the refraction index of encapsulant (typically EVA) is fairly similar to that of glass, the losses due to the glass–encapsulant interface will be considered negligible. Haedrich et al. [1] have estimated the other optical losses described above to be 1.1% abs.; in the same study the influence of the shadow projected by the tabbing ribbon onto the solar cell was also calculated, yielding a power loss of 0.32%. The radiation finally reaches the EVA–cell interface.

In order to minimize losses from reflection, the ARC layer possesses an intermediate index of refraction, the value of which lies between the indexes of glass and silicon. In particular, a silicon nitride ARC has a refractive index that varies between 1.985 and 2.167. As the cell is characterized in an air environment (with a refractive index of 1), the ARC contributes to reducing the index gap at the ARC and encapsulant interfaces, leading to a gain in power. This power gain results mainly from an increase in I_{sc}, which has been measured to be up to 5% compared with a bare cell (multicrystalline cell with a SiN_x coating [1])

Besides the optical gain due to refractive index coupling, as a result of encapsulation there are other optical considerations which contribute to an increase in module power [1,3,4,19]. For example, some PV glass producers have developed an ARC that is able to enhance the module power by

approximately 2%; the self-cleaning properties of these coatings, however, are usually inadequate once the modules are installed outdoors, offsetting the gain in power.

With some module producers another practice has been identified: in this case the PV modules are produced with the PV glass patterned surface facing the sun. The main purpose of the glass pattern, when it is oriented to the inner side of the module, is to achieve a good contact adherence between the glass and the encapsulant. When the patterned side of the glass is oriented outwards, there is a decrease in reflectance because of multiple reflections on its surface. To quantify the gain in power that is related exclusively to the 'misorientation' of the glass, several modules were produced with the same cells and materials; 50% of them were produced with the glass patterned side facing out, and then all the modules were measured at STC. An average of 2% power gain was measured for the modules with the patterned surface facing the sun. However, although this power gain is real, once the modules are installed outdoors there is a power decrease due to the self-cleaning difficulties of the sun-facing textured surface: this equates to a net loss of power for the final customer, who has indeed paid for that additional 2% of power increase.

"Once the modules are installed outdoors there is a power decrease due to the self-cleaning difficulties of the sun-facing textured surface."

Other gains are mainly derived from reflections on the tabbing ribbon and on the exposed backsheet where the cells are not present (i.e. cell spacing areas – see Fig. 15). The light reflected is directed to the glass–air interface and partially reflected back onto the cells.

In an attempt to quantify the power gain related exclusively to the cell spacing, two designs (A and B) of commercial modules were manufactured; the materials and processes were exactly the same. The modules were then measured at STC in a commercial solar simulator. The power gain derived from the back-reflected light has previously been calculated and measured, as reported in the literature [1,3,4]; in the current study, however, the power gain was found to be slightly better than the best results obtained by those researchers. Besides the backsheet reflection, other factors may be involved that explain an average power gain of 1% with a spacing increase of 1mm vertically and 0.5mm horizontally. From Fig. 16(b) it is seen that the increase in power is accompanied by a proportional increase in I_{sc}.

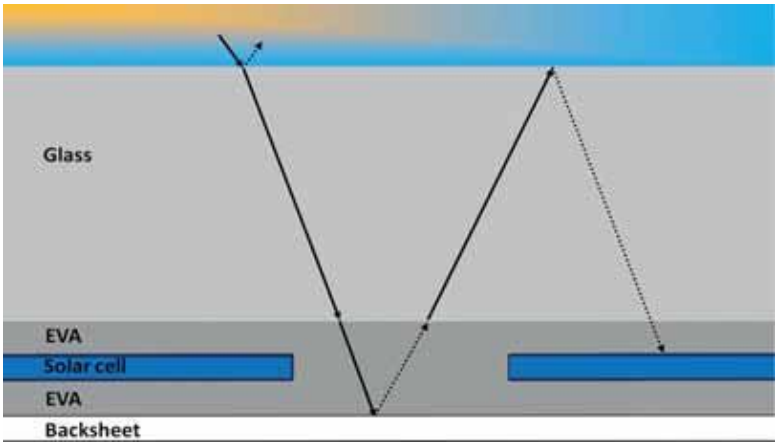

Figure 15. Sketch of the optical path related to backsheet reflections into the module.

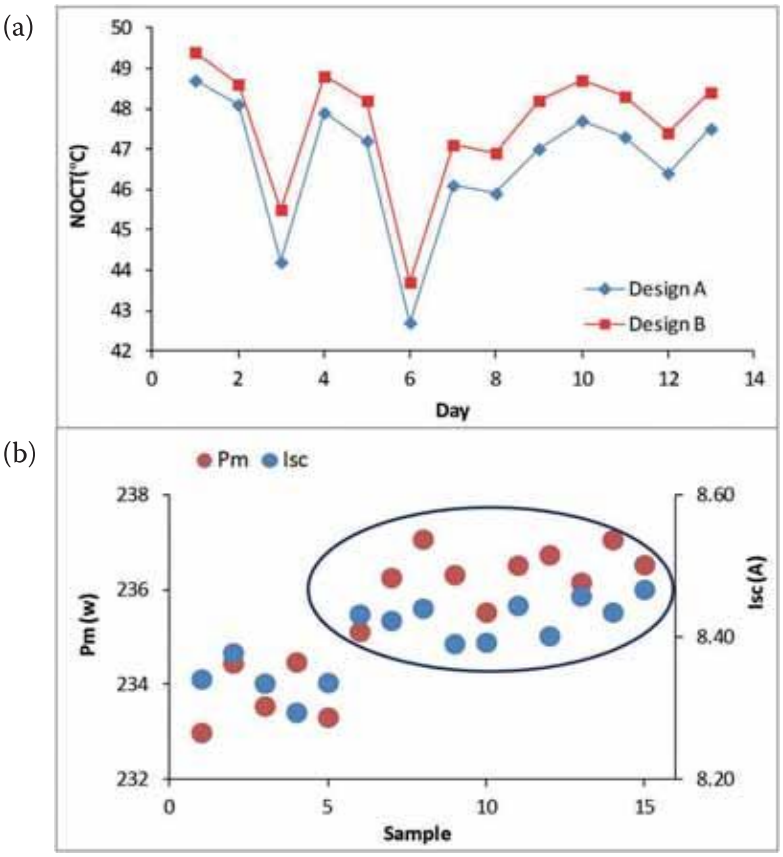

Figure 16. (a) NOCT results on different days for modules manufactured with two different designs. (b) Power and I_{sc} measurements for the two designs.

In addition to the benefit of a 1% power gain, there is another benefit, which is related to heat exchange with the environment. It is known that not all the irradiance absorbed by the PV module is convertible into electricity, but some of it is transformed into heat. The losses due to temperature are determined by the maximum

temperature coefficient γ, the approximate value of which for modules of crystalline silicon is –0.45%/°C. For example, for a PV module of 180Wp and an area of 1.3m^2 (nominal efficiency η_{STC} = 13.8%), encapsulated with glass (3.2mm) and an EVA backsheet, working at its maximum power point under an irradiance of 1,000W/m^2, thermal models [20] suggest a working temperature estimated at 48.7°C. This means, assuming the temperature coefficient given above, an actual efficiency given by $\eta_{48.7°C}$ = 13.8% × (1 – 23.7 × 0.0045) = 12.3%.

In actual operation, the temperature of the cell is determined by a balance of incoming and outgoing heat. On the one hand, it involves that portion of the irradiance which is not transformed into electricity but into heat in the interior of the cell. In this respect, it must be considered that a PV module with higher efficiency cells will transform a greater quantity of irradiance into electricity and less into heat; thus, if equality of all other construction features is assumed, the module's operating temperature will be lower. On the other hand, the dissipation of heat from the cell is limited by the encapsulation materials and module design. To investigate the second consideration, two modules, with designs A and B, were subjected to IEC 61215-10.6 [21] tests to determine the normal operation cell temperature (NOCT) on the CIEMAT electricity distribution network (Fig. 16(a)). Both modules were tested at the same time and together in the same rack. There is clear evidence that the NOCT of design A is around 1°C lower than that of design B.

Conclusions

This paper has presented an overview of all the various CTM losses. The sources of some of these losses have been investigated in an industrial environment; this may help the industry to avoid the losses, thus leading to a more efficient production of PV energy and a reduction in its cost. Finally, a different module design, aimed at increasing the output power, yielded a lower NOCT, with a consequent increase in the module's annual energy output.

Acknowledgements

The authors thank Aurinka PV Group for its support and materials in all the experiments carried out.

References

[1] Haedrich, I. et al. 2014, "Unified methodology for determining CTM ratios: Systematic prediction of module power", *Sol. Energy Mater. Sol. Cells*, Vol. 131, pp. 14–23.

[2] McIntosh, K.R. et al. 2009, "An optical comparison of silicon and EVA encapsulants for conventional silicon PV modules: A ray-tracing study", *Proc. 34th IEEE PVSC*, Philadelphia, Pennsylvania, USA.

[3] Ponce-Alcántara, S. et al. 2014, "The importance of optical characterization of PV backsheets in improving solar module power", *Photovoltaics International*, 26th edn, pp. 76–82.

[4] Sanchez-Illescas, P.J. et al. 2008, "Performance of photovoltaic modules with white reflective back sheets", *Proc. 23rd EU PVSEC*, Valencia, Spain.

[5] Wirth, H. et al. 2010, "Tabbing-stringing quality control challenges", *Photovoltaics International*, 9th edn, pp. 160–169.

[6] Evans, R. et al. 2015, "Simplified technique for calculating mismatch loss in mass production", *Sol. Energy Mater. Sol. Cells*, Vol. 134, pp. 236–243.

[7] Forniés, E. et al. 2013, "The influence of mismatch on relative power loss of photovoltaic modules", *Solar Energy*, Vol. 97, pp. 39–47.

[8] Chen, N. et al. 2013, "Assessing the impact of multi-busbars on metallization cost and efficiency of solar cells with digital inkjet-printed gridlines", *Proc. 10th HONET-CNS*, Magosa, Cyprus.

[9] Kaushika, N.D. & Rai, A.K. 2007, "An investigation of mismatch losses in solar photovoltaic cell networks", *Energy*, Vol. 32, pp. 755–759.

[10] Bucciarelli Jr, L.L. 1979, "Power loss in photovoltaic arrays due to mismatch in cell characteristics", *Solar Energy*, Vol. 23, pp. 277–278.

[11] Wilson, K. et al. 2006, "Measuring the effect of cell mismatch on module output", *Proc. 4th WCPEC*, Waikoloa, Hawaii, USA.

[12] Bishop, J.W. 1988, "Computer simulation of the effects of electrical mismatches in photovoltaic cell interconnection circuits", *Solar Cells*, Vol. 25, pp. 73–89.

[13] Lambarski, T.J. et al. 1981, "Effects of cells sorting and module matching on array output", *Proc. 15th IEEE PVSC*, Kissimmee, Florida, USA.

[14] Janoch, R. 1984, "Analysis of solar cell mismatch losses at standard and non-standard conditions", *Proc. 17th IEEE PVSC*, Kissimmee, Florida, USA.

[15] Wendt, J. et al. 2009, "The link between mechanical stress induced by soldering and micro damages in silicon solar cells", *Proc. 24th EU PVSEC*, Hamburg, Germany.

[16] de Jong, P.C. et al. 2005, "Low-stress interconnections for solar cells", *Proc. 20th EU PVSEC*, Barcelona, Spain.

[17] Zemen, Y. et al. 2013, "Comparison of new adhesives based on silver and carbon nanotubes for solar cells interconnection", *Sol. Energy Mater. Sol. Cells*, Vol. 109, pp. 155–159.

[18] Moyer, J. et al. 2010, "The role of silver contact paste on reliable connectivity systems", *Proc. 25th EU PVSEC*, Valencia, Spain.

[19] Zhichun, W.Q. et al. 2011, "Research on power loss of solar cell modules", *Photovoltaics International*, 12th edn, pp. 148–155.

[20] Silva, J.P. et al. 2010, "Spectral reflectance patterns of photovoltaic modules and their thermal effects", *J. Sol. Energy Eng.*, Vol. 132, No. 4, pp. 041016–041016-13.

[21] IEC 61215:2005 (10.6), "Crystalline silicon terrestrial photovoltaic (PV) modules – Design qualification and type approval".

About the Authors

Dr. Eduardo Forniés has a bachelor's degree and M.Sc. in applied physics from the Universidad Autónoma de Madrid, and received his Ph.D. in electronic engineering from the Universidad de Alcalá. Since 2001 he has worked in R&D departments of various companies (BP Solar, Pillar, Silicio Solar, ENSOL and Aurinka) with manufacturing experience in the whole value chain.

Dr. José P. Silva has a Ph.D. in PV systems engineering from the University of Jaén and a Bachelor of Engineering from the Polytechnic University of Madrid. After working as an electromechanical systems engineer, he became involved in R&D concerning the thermal behaviour of PV systems and their electrical characterization.

Enquiries

Dr. Eduardo Forniés
Aurinka PV Group SL
R&D Department
C/Marie Curie 19
28521 Madrid, Spain

Tel: +34 914 994 197
Email: efornies@aurinkapv.com / efornies@hotmail.com
Webpage: www.aurinkapv.com